

Raman Spectroscopic Study on the Hydration Structures of Tetraethylammonium Cation in Water

Takahiro Takekiyo* and Yukihiro Yoshimura

Department of Applied Chemistry, National Defense Academy, Yokosuka, Kanagawa 239-8686, Japan

Received: May 11, 2006; In Final Form: July 5, 2006

Conformational changes of tetraethylammonium ion (Et_4N^+) in aqueous solution have been studied by Raman spectroscopy as functions of pressure and concentration. The difference in the partial molar volume ($\Delta V^{g \cdot tg \rightarrow tt \cdot tt}$) between the *trans-gauche-trans-gauche* ($tg \cdot tg$) and *trans-trans-trans-trans* ($tt \cdot tt$) conformers of Et_4N^+ ion has been calculated from the pressure dependence of the relative Raman intensity ratio between the conformers. We discuss about the $\Delta V^{g \cdot tg \rightarrow tt \cdot tt}$ with two contributions from the molecular and hydration volumes. $\Delta V^{g \cdot tg \rightarrow tt \cdot tt}$ is found to be negative, and this is mainly due to the large molecular volume contribution. The value of $\Delta V^{g \cdot tg \rightarrow tt \cdot tt}$ becomes smaller with increasing R probably due to the hydration volume contribution. In view of the pressure and concentration dependences, the water molecules around Et_4N^+ ions at $R = 19$ ($R = \text{moles of water/moles of salt}$) mainly form the hydrophobic hydration. The hydrophobic hydration may prefer the $tt \cdot tt$ conformer to the $tg \cdot tg$ conformer. On the other hand, the hydration structure at $R = 4$ no longer forms the hydrophobic hydration and changes to another type of hydration, where the medium H-bond component is the dominant species. The increase of the ion-ion interactions with decreasing R induces large fractions of the $tg \cdot tg$ conformer.

1. Introduction

Hydrophobic hydration plays an important role in the thermodynamic and solution properties of aqueous apolar solutes and the stabilization of proteins in aqueous solution.^{1–4} Tetraalkylammonium halides have long been considered as model systems to investigate the nature of hydrophobic hydration because of their good solubility in aqueous solution and their nonpolar surface which increases with increasing alkyl-chain length within the series of homologues.^{5–17} These compounds also provide a suitable candidate for investigating the competing influence of the Coulombic effect of the charge density and the hydrophobic effect of the nonpolar surface.^{18,19}

There have been some reports on the effect of R_4NX on the structural stability of proteins.^{20–22} In the recent calorimetric study by Jain and Ahluwalia,²² the R_4NX destabilizes proteins by interacting with the exposed hydrophobic groups of the denatured state and simultaneously weakening the hydrophobic interactions between the nonpolar groups of the protein. The destabilization of protein by R_4NX becomes stronger with increasing alkyl chain. However the details of the destabilizing effect of additives are unclear because of the complicated interactions among the R_4NX , proteins, and water molecules. Therefore, as a first step, it is important to investigate the relationship between the R_4N^+ ion and water molecules at the microscopic molecular level such as conformational equilibria under various conditions.

Here, we focused on the aqueous tetraethylammonium halides (Et_4NX) solution, having an intermediate character of the electrostatic and hydrophobic interactions. The interesting feature is that Et_4NX salts show the conformational equilibria between the *trans-trans-trans-trans* ($tt \cdot tt$) and *trans-gauche-trans-gauche* ($tg \cdot tg$) conformers for the rotation of Et-N^+-

Et axis in the aqueous solution.^{23,24} Figure 1 shows the $tg \cdot tg$ and $tt \cdot tt$ conformers of Et_4N^+ ion to illustrate what these conformers look like.

Although it has been considered that the hydration structure around Et_4N^+ ion mainly forms the hydrophobic hydration,^{18,19} Conway and Verrall²⁵ reported that the water molecules around Et_4N^+ ion form the electrostatic hydration. Hertz et al.²⁶ showed the cation-cation interaction (the dimerization of cations) exists in the high salt concentrations and this interaction becomes stronger with decreasing water concentration. Moreover, they concluded that the hydration structure around Et_4N^+ ion at high salt concentrations is different from that at low salt concentrations.

From the pressure effect on the hydrophobic hydration structure around a nonpolar solute, Sawamura et al.^{27,28} found that the hydration water is not compressed more than bulk water. From the viewpoint of the isothermal compressibility, which is the physical quantity of the pressure derivative of partial molar volume (PMV), the differences in the isothermal compressibilities between the bulk water and water around the nonpolar solute reflect the hydrophobic hydration. This effect is enhanced to appear at higher pressures and lower temperatures. Imai and Hirata²⁹ supported the experimental results of Sawamura et al. by RISM theoretical study.

In viewing of these results, the study on the pressure effect on the conformational equilibria of Et_4N^+ ion as a function of concentration might provide the information about the difference in the hydration structures around Et_4N^+ ion between at high and low salt concentrations.

In this study, we have observed the Raman spectral changes in the CH_3 rocking and uncoupled OD stretching modes of the aqueous Et_4NBr solution as functions of pressure and water concentration. The difference in the PMV between the conformers of Et_4N^+ ion is determined.

* Corresponding author. Telephone: +81-46-841-3810. Fax: +81-46-844-5901. E-mail: take214@nda.ac.jp.

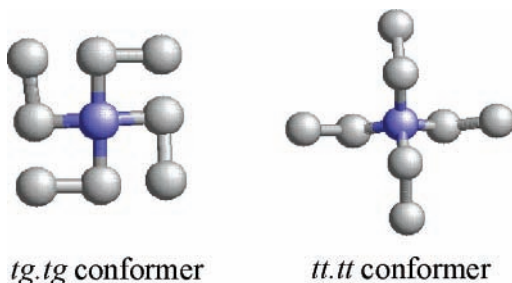


Figure 1. Schematic representation for the structures of the *trans-gauche-trans-gauche* (*tg·tg*) and *trans-trans-trans-trans* (*tt·tt*) conformers of Et_4N^+ ion.

2. Materials and Methods

Tetraethylammonium bromide (Et_4NBr) was obtained from Tokyo Kasei Industry Co. Ltd. All sample solutions were prepared by dissolving the vacuum-dried Et_4NBr in 5% D_2O solution (purity of $\text{D}_2\text{O} > 99.8\%$) as a solvent. The concentrations of all the solutions are expressed by R (=moles of water/moles of salt).

Raman spectra were measured by a JASCO NR-1800 Raman spectrophotometer equipped with a single monochromator and a CCD detector. The exposure time of each run was 300 s. The 514.5 nm line from a Lexel Ar^+ ion laser was used as an exacting source with a power of 350 mW. For the high-pressure experiments, we used a diamond anvil cell (DAC). The sample solutions were placed together with a small amount of powdered ruby chip in a SUS301 gasket mounted on the DAC. The ruby chip was used for a pressure calibrant.^{30–32} All the measurements were made at a room temperature (298 K).

The molecular volume (V_M) can be obtained from the geometric volume calculation. The V_M is composed of the van der Waals volume (V_w) and the void volume (V_v); $V_M = V_w + V_v$. The V_w is the volume occupied by the van der Waals spheres representing atoms. The V_v is defined as void space inside the solute molecule or at its surface that the solvent probe cannot access. The V_M of Et_4NBr was calculated using the Alpha-Shapes program,^{33,34} which enables calculation of the solvent accessibility of the molecular surface by assuming that Et_4NBr is a hard-sphere probe. The radius of a probe of Et_4NBr was defined as 5.95 Å, taking account of the ion-ion interactions such as ion-pairs and cation-cation interactions. We used the optimized structures of the *tt·tt* and *tg·tg* conformers for Et_4N^+ ion at the B3LYP/6-31G+(d,p) level to calculate the V_M .³⁵

3. Results and Discussion

Figure 2 shows the representative Raman spectral changes in the CH_3 rocking mode of Et_4NBr in aqueous solution as a function of pressure. The assignments of Raman modes of each conformer have been described elsewhere.^{23,24} With increasing pressure, the relative Raman intensity of the *tt·tt* conformer increases (the *tg·tg* conformer decreases). This behavior is common to all the concentrations studied ($R = 4$ –19). Although all the experiments were performed with the solutions of high salt concentrations, the Raman spectra, even at $R = 4$, do not show any spectral features of the glassy state and also those of the crystalline state upon compression.²⁴

Figure 3 shows the pressure dependence of the relative Raman intensity ratio between the *tg·tg* and *tt·tt* conformers at various concentrations. We determined ΔV between the conformers from the pressure dependence of the relative Raman intensities. Assuming that the ratio of the Raman scattering cross-sections

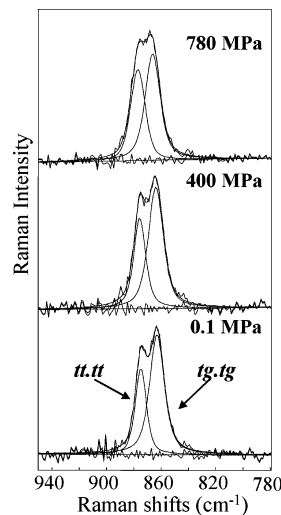


Figure 2. *In situ* Raman spectral changes in the CH_3 rocking mode of Et_4NBr in aqueous solution as a function of pressure at $R = 19$.

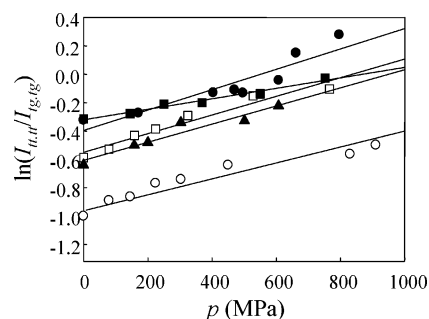


Figure 3. Pressure dependences of $\ln(I_{tt·tt}/I_{tg·tg})$ of the CH_3 rocking band of Et_4NBr in aqueous solution at various concentrations. The symbols of \bullet , \square , \blacktriangle , \circ , and \blacksquare represent $R = 4, 6, 10, 11,$ and 19 , respectively. The lines are the results of the least-squares analysis.

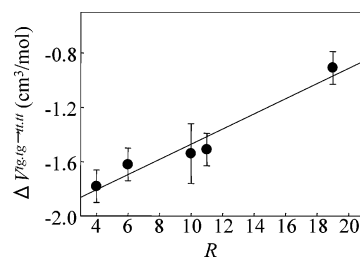


Figure 4. Concentration dependence of the $\Delta V^{tg·tg-tt·tt}$ of Et_4N^+ ion in aqueous Et_4NBr solution. The line is the result of the least-squares analysis.

between the conformers is independent of a pressure,³⁶ $\Delta V^{tg·tg-tt·tt}$ is given by

$$\Delta V^{tg·tg-tt·tt} = -RT \left\{ \frac{\partial \ln \left(\frac{I_{tt·tt}}{I_{tg·tg}} \right)}{\partial p} \right\}_T \quad (1)$$

where R , T , and p are gas constant, temperature, and pressure, respectively. $I_{tt·tt}$ or $I_{tg·tg}$ indicates the relative Raman intensity of each conformer. According to eq 1, we obtained $\Delta V^{tg·tg-tt·tt}$ for Et_4NBr .

Figure 4 shows the concentration dependence of the $\Delta V^{tg·tg-tt·tt}$. It is found that the PMV of the *tt·tt* conformer is smaller than that of the *tg·tg* conformer throughout the studied concentration ranges. It is also noticed that the absolute value of $\Delta V^{tg·tg-tt·tt}$ becomes smaller with increasing R (increasing water concentration).

TABLE 1: Concentration Dependences of the Volume Difference from the *tg*·*tg* to *tt*·*tt* Conformers of Et₄N⁺ Ion in Aqueous Et₄NBr Solution

R	volume (cm ³ /mol)		
	$\Delta V_{M}^{tg \cdot tg \rightarrow tt \cdot tt}$	$\Delta V_{M}^{tg \cdot tg \rightarrow tt \cdot tt_a}$	$\Delta V_{hyd}^{tg \cdot tg \rightarrow tt \cdot tt}$
4	-1.78 ± 0.19	-1.34	-0.44
6	-1.62 ± 0.12	-1.34	-0.28
10	-1.54 ± 0.14	-1.34	-0.20
11	-1.51 ± 0.15	-1.34	-0.17
19	-0.91 ± 0.09	-1.34	+0.43

*Alpha-Shapes program.

For further discussions, we decomposed $\Delta V_{M}^{tg \cdot tg \rightarrow tt \cdot tt}$ into two terms³⁷ as follows:

$$\Delta V_{M}^{tg \cdot tg \rightarrow tt \cdot tt} = \Delta V_{M}^{tg \cdot tg \rightarrow tt \cdot tt_a} + \Delta V_{hyd}^{tg \cdot tg \rightarrow tt \cdot tt} \quad (2)$$

where ΔV_M is the difference between the molecular volumes of the conformers. ΔV_{hyd} is the hydration volume difference, which results from a change in the intermolecular interaction between the solute and solvent. We obtained the value of -1.34 cm³/mol as ΔV_M by the Alpha-Shapes program.^{33,34} Thus, we can obtain ΔV_{hyd} from eq 2. The estimated volume contributions of Et₄N⁺ ion are listed in Table 1. Clearly, the smaller PMV of the *tt*·*tt* conformer of Et₄N⁺ ion is mainly due to the large molecular volume contribution.

In previous Raman studies, it was reported that $\Delta V_{gauche(cis) \rightarrow trans}$ of simple organic compounds such as chloroacetone (CA)³⁸ and 2-chloroacetamide (MCA)³⁶ in water are -0.9 ± 0.4 cm³/mol for CA and -1.5 ± 0.3 cm³/mol for MCA. The smaller PMVs of the *trans* conformer of CA and MCA are mainly ascribed to the smaller hydration volume (ΔV_{hyd}). These volume changes of the simple organic compounds are the same order of $\Delta V_{M}^{tg \cdot tg \rightarrow tt \cdot tt}$ of Et₄N⁺ ion, but the origin of the volume change for the simple organic compounds is different from that for Et₄N⁺ ion.

Here we must mention about the large difference in the ΔV_{hyd} values of Et₄N⁺ ion at *R* = 4 and 19; i.e., the sign of ΔV_{hyd} of Et₄N⁺ ion at *R* = 4 changes to plus at *R* = 19. This means that the hydration volume of the *tg*·*tg* conformer at *R* = 4 is larger than that of the *tt*·*tt* conformer, but the situation becomes reverse at *R* = 19. We speculate that the difference in the $\Delta V_{M}^{tg \cdot tg \rightarrow tt \cdot tt}$ values of Et₄N⁺ ion between *R* = 4 and 19 mainly comes from the difference in the hydration structures around Et₄N⁺ ion. To discuss more about the values of the hydration volume at *R* = 4 and 19, it is necessary to clarify the difference in the hydration structures of Et₄N⁺ ion.

There have been a number of reports on the hydration number of Et₄N⁺ ion. Recently, Pottela and Lossen³⁹ calculated the hydration number of Et₄N⁺ ion to be 21 by an NMR study. On the other hand, Hertz et al.²⁸ assigned this number to be 30. Although there are some scatterings in the hydration numbers, it is clear that the number of water molecules per an Et₄N⁺ ion is insufficient to form the complete hydration shell around the Et₄N⁺ ion in the concentration range from *R* = 4 to 19. According to the high-pressure NMR relaxation study by Liegel et al.,⁴⁰ the insufficient water molecules around Et₄N⁺ ion at $\sim R = 20$ induce the formation of the hydrophobic hydration. Kuhnelt and Kaatze⁴¹ determined the isotropic compressibility (κ) of aqueous Et₄NBr solution at various concentrations by ultrasonic absorption. The value of κ of aqueous Et₄NBr solution becomes smaller with increasing salt concentration. They concluded that the smaller κ with increasing salt concentration is due to the cation-cation interactions. Therefore, it is most likely that the hydration structure around Et₄N⁺ ion at *R* = 19

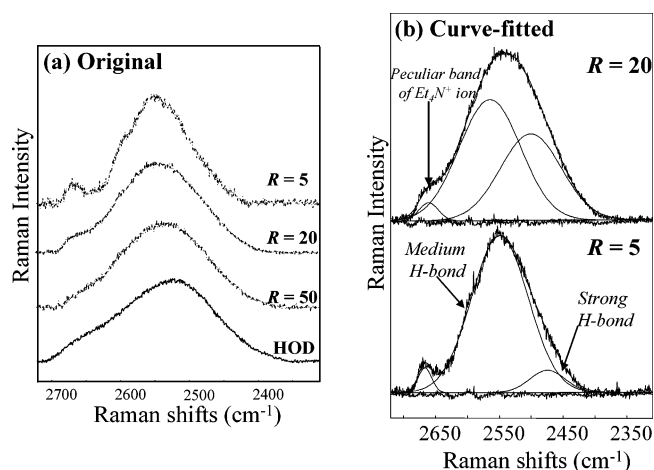


Figure 5. (a) Original and (b) curve-fitted Raman spectra of the uncoupled OD stretching mode of aqueous Et₄NBr solution at various concentrations.

mainly forms the hydrophobic hydration. Our results in Table 1 reveal that the hydration volume due to the hydrophobic hydration around the *tt*·*tt* conformer at *R* = 19 is larger than that around the *tg*·*tg* conformer. However we must mention that the direct correlation between the PMV and compressibility of aqueous Et₄NBr solution is not well-defined. Additionally the PMVs of alcohols in the alcohol-water systems are often nonmonotonic (initially decrease with increasing concentration and then increase).⁴² There may be a possibility that the PMV of the aqueous Et₄NBr solution contains such a feature intrinsically.

It is difficult to say more about the hydration structure at *R* = 4. Thus, as a next step, we investigated the concentration dependence of the Raman uncoupled OD stretching spectra of aqueous Et₄NBr solution to elucidate the hydration structure around Et₄N⁺ ion at *R* = 4.

Figure 5 shows the changes in the (a) original Raman spectra and (b) their curve-fitted spectra of the uncoupled OD stretching mode in aqueous Et₄NBr solution at various concentrations. The observed spectra were able to be fitted well by two components, though there may be the OD band species stretching modes in aqueous solution. In previous Raman studies, Kanno et al.⁴³⁻⁴⁵ decomposed the Raman uncoupled OD stretching bands of aqueous electrolyte solutions into two Gaussian-Lorentzian mixed functions, the low- and high-wavenumber components. As well as the analysis by Kanno et al., Stangret and Gampe^{46,47} decomposed the uncoupled IR OD stretching bands of aqueous electrolyte solutions into two components in an attempt to discuss the ion hydration. Corcelli and Skinner⁴⁸ also supported the two species model of the water structure by the IR and Raman spectra of HOD in water.

However there is an alternative view that the isolated Raman OD band species of pure liquid water is better described by a continuum of water structures, rather than by two or more species with different types of hydrogen bonding structure.⁴⁹ Thus, the discussions on the water structure whether we should stand on the continuum model or the two or more species model are still under debate.

For the present, we used the two species analysis for the behavior of the water molecule around Et₄N⁺ ion. That is, the low- and high-wavenumber components represent the fractions of the strong and medium hydrogen bond (H-bond) components in the solution, respectively. It is to be noted that the results obtained are sensitive to the nature of the approximations made in decomposing the spectra. Therefore we tried to check the

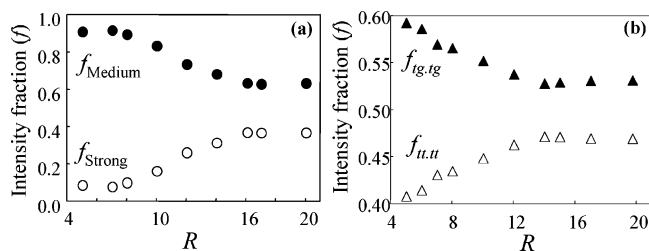


Figure 6. Concentration dependences of the intensity fractions for (a) the strong and medium H-bond components and (b) the $tg*tg$ and $tt*tt$ conformers of Et_4N^+ ion in aqueous solution at 0.1 MPa. The symbols of \bullet and \circ represent the intensity fractions of the medium, strong H-bond components, \blacktriangle and \triangle show those of the $tg*tg$ and $tt*tt$ conformers, respectively.

degree to which the results change quantitatively when other band-shape functions are used to decompose the spectra. Here, to examine the model function dependence of the spectral decomposition, we analyzed the Raman bands of aqueous Et_4NBr solution by three functions; the Gauss, Gaussian–Lorentzian mixed, and Voigt functions.⁵⁰ As an indicator of the accuracy of the band deconvolution procedure, we used a reduced χ (χ^2), which represents the parameter of the goodness-of-fit. The smaller the value of χ^2 , the better the fitting precision of the spectral decomposition. The χ^2 values of three functions are 1.47 ± 0.15 for the Gauss function, 1.42 ± 0.09 for the Gaussian–Lorentzian mixed function, and 1.52 ± 0.13 for the Voigt function, respectively. We note that the χ^2 value of the Gaussian–Lorentzian mixed function is the smallest, but three functions show almost the same values. Thus different choices do not change the general trends in the results. We applied the results of Gaussian–Lorentzian mixed function to the spectral analysis.

We estimated the intensity fractions (f) of the strong (f_{strong}) and medium (f_{medium}) H-bond components given by

$$f_{\text{strong}} = \frac{I_{\text{strong}}}{I_{\text{strong}} + I_{\text{medium}}}, \quad f_{\text{medium}} = \frac{I_{\text{medium}}}{I_{\text{strong}} + I_{\text{medium}}} \quad (3)$$

where I_{strong} and I_{medium} represent the relative Raman intensities of the strong and medium H-bond components, respectively. The concentration dependences of the intensity fractions (f) of the strong (f_{strong}) and medium (f_{medium}) H-bond components of the uncoupled OD stretching mode are shown in Figure 6(a). It is remarkable that the f_{medium} decreases (the f_{strong} increases) with increasing water concentration from $R = 8$ to 16 and then remains constant up to $R = 20$. It is also noticed that the f_{medium} is dominant at around $R = 4$, whereas the f_{strong} is comparable to the f_{medium} at around $R = 19$.

To proceed further, we compared the concentration dependences of the intensity fractions f_{strong} and f_{medium} with those of the $tg*tg$ and $tt*tt$ conformers of Et_4N^+ ion for the CH_3 rocking band.²⁴ It is remarkable that the concentration dependences of the f_{medium} and f_{strong} are fairly consistent with those of the f_{tg*tg} and f_{tt*tt} of Et_4N^+ ion. Thus, it is likely that the hydration structures around the $tt*tt$ and $tg*tg$ conformers of the Et_4N^+ ion correlate with the strong and medium H-bond components, respectively. It seems that the hydration structure at $R = 4$, where the medium H-bond is a main component, prefers the $tg*tg$ conformer to the $tt*tt$ conformer. We speculate that the ion–ion interactions, e.g., cation–cation, induce a large fraction of the $tg*tg$ conformer in the solution. In the present experimental conditions, the ion–pair between Et_4N^+ and Br^- would also play an important role in the hydrational and conformational behavior of a solute ion. The change of the sign of ΔV_{hyd} with

decreasing R (increasing the ion–ion interactions) supports the speculation that the hydrophobic hydration around Et_4N^+ ion changes to another hydration structure at higher salt concentrations.

4. Conclusions

The Raman spectra of Et_4NBr in aqueous solution have been measured as functions of pressure and water concentration. We discussed the hydration structures around Et_4N^+ ion in view of the conformational equilibria of Et_4N^+ ion.

We found that the increase of the ion–ion interactions such as ion–pairs and cation–cation ones induces large fractions of the $tg*tg$ conformer and the medium H-bond component in the solution. We suggest that the hydrophobic hydration may prefer the $tt*tt$ conformer to the $tg*tg$ conformer at $R = 19$, and the hydration structure around Et_4N^+ ion at $R = 4$ might be different from the hydrophobic hydration. The concentration dependence of ΔV_{tg*tg}^{tt*tt} also implies the change of the hydration structures around Et_4N^+ ion. More continuous experimental and theoretical studies will give us further knowledge for understanding the effect of R_4N^+ ion, e.g., on the structural stability of proteins.

References and Notes

- (1) Franks, F., Ed. *A Comprehensive Treatise*; Plenum: New York, 1972–1982; Vols. 1–7.
- (2) Tanford, C. *The Hydrophobic Effect: Formation of Micelles and Biological Membranes*; Wiley-Interscience: New York, 1980.
- (3) Ben-Naim, A. *Hydrophobic Interaction*; Plenum: New York, 1980.
- (4) Pratt, L. R. *Annu. Rev. Phys. Chem.* **1985**, *36*, 433.
- (5) Kucas, M.; Tronriand, A. D.; Ceccaldi, M. *J. Phys. Chem.* **1975**, *79*, 913.
- (6) Jolicoeur, C.; Paquette, J.; Lucas, M. *J. Phys. Chem.* **1978**, *82*, 1051.
- (7) Kanno, H.; Shimada, K.; Yoshino, K.; Iwamoto, T. *Chem. Phys. Lett.* **1984**, *112*, 242.
- (8) Eriksson, P. O.; Lindblom, G.; Burnell, E. E.; Tiddy, G. T. J. *J. Chem. Soc., Faraday Trans. 1* **1988**, *84*, 3129.
- (9) Holz, M.; Patil, K. J. *Ber. Bunsenges. Phys. Chem.* **1991**, *95*, 107.
- (10) Fawcett, W. R.; Fedurco, M.; Opallo, M. *J. Phys. Chem.* **1992**, *96*, 9959.
- (11) Bradl, S.; Lang, E. W. *J. Phys. Chem.* **1993**, *97*, 10463.
- (12) Ohnishi, A.; Kanno, H. *J. Solution Chem.* **1996**, *25*, 279.
- (13) Ohnishi, A.; Kanno, H. *Chem. Phys. Lett.* **1996**, *263*, 259.
- (14) Slusher, J. T.; Cummings, P. T. *J. Phys. Chem. B* **1997**, *101*, 3818.
- (15) Sun, J.; Forsyth, M.; MacFarlane, D. R. *J. Phys. Chem. B* **1998**, *102*, 8858.
- (16) Yoshimura, Y.; Ohnishi, A.; Kanno, H. *J. Sol. Chem.* **1999**, *28*, 1127.
- (17) Kuba, A.; Hawlicka, E. *Phys. Chem. Chem. Phys.* **2003**, *5*, 4858.
- (18) Wen, W. Y.; Horne, R. A., Eds. *Water and Aqueous Solutions*; Wiley: New York, 1972; p 613.
- (19) Wen, W. Y. *J. Solution Chem.* **1973**, *2*, 253.
- (20) von Hippel, P. H.; Wong, K.-Y. *J. Biol. Chem.* **1965**, *240*, 3909.
- (21) Gerlisma, G. Y. *J. Biol. Chem.* **1968**, *243*, 957.
- (22) Jain, S.; Ahluwalia, J. C. *Biophys. Chem.* **1996**, *59*, 171.
- (23) Naudin, C.; Bonhomme, F.; Bruneel, J. L.; Grondin, D. J.; Lassegues, J. C.; Sevant, L. *J. Raman Spectrosc.* **2000**, *31*, 979.
- (24) Takekiyo, T.; Yoshimura, Y. *Chem. Phys. Lett.* **2006**, *420*, 8.
- (25) Conway, B. E.; Verrall, R. E. *J. Phys. Chem.* **1966**, *70*, 3952.
- (26) Hertz, H. G.; Lindman, B.; Siepe, V. *Ber. Bunsenges. Phys. Chem.* **1969**, *73*, 234.
- (27) Sawamura, S.; Kitamura, K.; Taniguchi, Y. *J. Phys. Chem.* **1989**, *93*, 4931.
- (28) Sawamura, S.; Nagaoka, K.; Machikawa, T. *J. Phys. Chem. B* **2001**, *105*, 2429.
- (29) Imai, T.; Hirata, F. *J. Chem. Phys.* **2005**, *122*, 094509.
- (30) Chervin, J. C.; Canny, B.; Guthier, M.; Pruzan, Ph. *Rev. Sci. Instrum.* **1993**, *64*, 203.
- (31) Mao, H. K.; Bell, P. M.; Shaner, J. W.; Steinberg, D. J. *J. Appl. Phys.* **1978**, *49*, 3276.
- (32) Mao, H. K.; Xu, J.; Bell, P. M. *J. Geophys. Res.* **1986**, *91*, 4673.
- (33) Liang, J.; Edelsbrunner, H.; Fu, P.; Sudhakar, P. V.; Subramaniam, S. *Proteins* **1998**, *33*, 1.
- (34) Liang, J.; Edelsbrunner, H.; Fu, P.; Sudhakar, P. V.; Subramaniam, S. *Proteins* **1998**, *33*, 18.
- (35) Frisch, M. J.; Trucks, G. W.; Schlegel, H. B.; Scuseria, G. E.; Robb, M. A.; Cheeseman, J. R.; Zakrzewski, V. G.; Montgomery, J. A.; Daniels,

- A. D.; Kudin, K. N.; Strain, M. C.; Farkas, O.; Tomasi, J.; Barone, V.; Cossi, M.; Cammi, R.; Mennucci, B.; Pomelli, C.; Adamo, C.; Clifford, S.; Ochterski, J.; Petersson, G. A.; Ayala, P. Y.; Cui, Q.; Morokuma, K.; Malick, D. K.; Rabuck, A. D.; Raghavachari, K.; Foresman, J. B.; Cioslowski, J.; Ortiz, J. V.; Baboul, A. G.; Stefanov, B. B.; Liu, G.; Liashenko, A.; Piskorz, P.; Komaromi, I.; Gomperts, R.; Martin, R. L.; Fox, D. J.; Kieth, T.; Al-Laham, M. A.; Peng, C. Y.; Nanayaakkara, A.; Gonzalez, C.; Challacombe, M. P.; Gill, M. W.; Johnson, B.; Chen, W.; Wong, M. W.; Andres, J. L.; Gonzalez, C.; Head-Gordon, M.; Replogle, E. S.; Pople, J. A. *GAUSSIAN 98*; Gaussian, Inc.: Pittsburgh, PA, 2003.
- (36) Takekiyo, T.; Kato, M.; Taniguchi, Y. *J. Solution Chem.* **2004**, *33*, 761.
- (37) Takekiyo, T.; Shimizu, A.; Kato, M.; Taniguchi, Y. *Biochim. Biophys. Acta* **2005**, *1750*, 1.
- (38) Shiratori, Y.; Namba, Y.; Kato, M.; Taniguchi, Y. *Bull. Chem. Soc. Jpn.* **2003**, *76*, 501.
- (39) Pottel, R.; Lossen, D. *Ber. Bunsen-Ges. Phys. Chem.* **1967**, *71*, 135.
- (40) Liegel, B.; Bradl, S.; Schatz, T.; Lang, E. W. *J. Phys. Chem.* **1996**, *100*, 897.
- (41) Kuhnel, V.; Kaatze, U. *J. Phys. Chem.* **1996**, *100*, 19747.
- (42) González-Salgado, D.; Nezbeda, I. *Fluid Phase Equilib.* **2006**, *240*, 161.
- (43) Kanno, H.; Ohnishi, A.; Tomikawa, K.; Yoshimura, Y. *J. Raman Spectrosc.* **1999**, *30*, 705.
- (44) Hidata, F.; Kanno, H. *Chem. Phys. Lett.* **2003**, *379*, 216.
- (45) Kanno, H.; Yonehama, K.; Somraj, A.; Yoshimura, Y. *Chem. Phys. Lett.*, in press.
- (46) Stangret, J.; Gampe, T. *J. Phys. Chem. B* **1999**, *103*, 3778.
- (47) Stangret, J.; Gampe, T. *J. Phys. Chem. A* **2002**, *106*, 5393.
- (48) Corcelli, S. A.; Skinner, J. L. *J. Phys. Chem. A* **2005**, *109*, 6154.
- (49) Smith, J. D.; Cappa, C. D.; Wilson, K. R.; Cohen, R. C.; Geissler, P. L.; Saykally, R. J. *Proc. Natl. Acad. Sci. U.S.A.* **2005**, *102*, 14171.
- (50) *GRAMS/386 User's Guide*; Galacteric Industries.: NH, p 170.